

The dependence on atmospheric resolution of ENSO and related East Asian-western North Pacific summer climate variability in a coupled model

Bo Liu^{1,2} · Guijie Zhao³ · Gang Huang^{1,2,4} · Pengfei Wang^{1,5} · Bangliang Yan⁵

Received: 22 March 2017 / Accepted: 14 August 2017 / Published online: 24 August 2017
© Springer-Verlag GmbH Austria 2017

Abstract The authors present results for El Niño-Southern Oscillation (ENSO) and East Asian-western North Pacific climate variability simulated in a new version high-resolution coupled model (ICM.V2) developed at the Center for Monsoon System Research of the Institute of Atmospheric Physics (CMSR, IAP), Chinese Academy of Sciences. The analyses are based on the last 100-year output of a 1000-year simulation. Results are compared to an earlier version of the same coupled model (ICM.V1), reanalysis, and observations. The two versions of ICM have similar physics but different atmospheric resolution. The simulated climatological mean states show marked improvement over many regions, especially the tropics in ICM.V2 compared to those in ICM.V1. The common bias in the cold tongue has reduced, and the warm biases along the ocean boundaries have improved as well. With improved simulation of ENSO, including its period and strength, the ENSO-related western North Pacific summer climate variability becomes more realistic compared to the observations. The simulated East Asian

summer monsoon anomalies in the El Niño decaying summer are substantially more realistic in ICM.V2, which might be related to a better simulation of the Indo-Pacific Ocean capacitor (IPOC) effect and Pacific decadal oscillation (PDO).

1 Introduction

There is a developing demand for more accurate climate predictions with models that contain more detailed physical, chemical, and biological processes. To meet this demand, an improved higher-resolution model is often considered as one approach. Williamson et al. (1995) obtained a significant improvement in the model performance when the horizontal resolution changes from T21 to T42 in a spectral model but small improvement when the resolution increases from T42 to T216. Sensitive experiments have been conducted with a global climate model (GCM) to examine the impacts of the spatial resolution on the model performance. Roeckner et al. (2006) found that ECHAM5 does not bring a more realistic climate state when the horizontal resolution increases from T42 to T159, while the simulations improve with vertical levels increasing from 19 to 31. Using the new version ECHAM6, Hertwig et al. (2015) analyzed the effect of the horizontal resolution on the simulation of the mean climate state and climate variability. They stated that the biases of simulations, including the mean state and the variance, reduce with the increase of the horizontal resolution, especially in extra-tropical troposphere, but the simulation of precipitation is still a major problem. Owing to the great development of computation power, previous studies have the opportunity to test the results of coupled models with much higher resolution. Sakamoto et al. (2012) showed improved simulations, especially in orographic effects and coastal upwelling, with a high-resolution coupled model. Gent et al. (2010) demonstrated great improvements in mean state using

✉ Gang Huang
hg@mail.iap.ac.cn

¹ State Key Laboratory of Numerical Modeling for Atmospheric Sciences and Geophysical Fluid Dynamics, Institute of Atmospheric Physics, Chinese Academy of Sciences, Beijing 100029, China

² College of Earth Science, University of Chinese Academy of Sciences, Beijing 100049, China

³ Beijing Meteorological Service, Beijing 100089, China

⁴ Joint Center for Global Change Studies, Beijing 100875, China

⁵ Center for Monsoon System Research, Institute of Atmospheric Physics, Chinese Academy of Sciences, Beijing 100029, China

the National Center for Atmospheric Research (NCAR) Community Climate System Model (CCSM) with an atmospheric resolution of 0.5° . In addition, other researchers obtain improvements in different aspects in different CCSM versions with higher resolution (Bryan et al. 2010; McClean et al. 2011). Delworth et al. (2012) presented results of different versions of GFDL coupled model with the horizontal resolution ranging from 200 to 50 km. The results show marked improvement of simulations over many regions, especially the tropics where there are strong atmosphere-ocean interactions.

However, simulations with higher-resolution models, especially coupled models, will increase dramatically the cost of computations. In order to achieve the specific goals, the balance between resolution and computation should be taken into consideration. On the other side, there is indication that increasing resolutions have minor benefits (Williamson et al. 1995; Roeckner et al. 2006). Thus, some coarse-resolution model is still used in the scientific researches owing to the small computation time.

In the goal of predicting the seasonal climate anomaly over the East Asian-western North Pacific (EA-WNP), especially the East Asian summer monsoon (EASM), a coupled model, called the integrated coupled model (ICM), has been developed (Huang et al. 2014). EASM is a dominant climate system in the EA-WNP, which has great social and economic influences (Rodwell and Hoskins 2001; Jiang et al. 2008; Hu et al. 2013). Many researches have indicated that the El Niño-Southern Oscillation (ENSO) has a large impact on the EASM in the following summer through an anomalous anticyclone/cyclone over the western North Pacific (WNP) (Zhang et al. 1999; Wang et al. 2000, 2003). During the El Niño mature phase, Wang et al. (2000) proposed the local wind-evaporation (WES) feedback mechanism is the key process to maintain the anomalous anticyclone over the WNP. Moreover, many other researches tend to emphasize the role of the tropical Indian Ocean warming (Yang et al. 2007; Wu et al. 2009; Xie et al. 2009). These two mechanisms are combined and named as the Indo-western Pacific Ocean capacitor (IPOC) effect by Xie et al. (2016); they mentioned both mechanisms are available just in a two-stage evolution. In order to predict the EASM, the status of the relationship between ENSO and EASM is of major significance. However, the relationship is unstable (Wang 2002) and impacted by many factors, such as Indian Ocean warming (Hu et al. 2013), the Pacific decadal oscillation (PDO; Mantua et al. 1997), and so on. For example, Feng et al. (2014) mentioned the PDO in a different phase may modulate the ENSO-EASM relationship through the decay speed of El Niño during 1957–2011. Moreover, the climate model is a useful tool to study the relationship between the ENSO and the EASM. Using a preindustrial control simulation from CCSM4, Song and Zhou (2015) found the ENSO-EASM relationship is modulated by the PDO.

The purpose of this paper is to examine the effect of atmospheric horizontal resolution on the performance of the ICM. For that purpose, we compare the simulations of the ICM with two different horizontal resolutions of the atmospheric model: T31 ($3.75^\circ \times 3.75^\circ$) and T63 ($1.8^\circ \times 1.8^\circ$). Except for the atmospheric horizontal resolution, the rest of the model, including the ocean portion and physic processes, is the same. We want to know whether the biases of mean climate states and the variability decrease with the increase of atmospheric horizontal resolution in the coupled model simulation.

The model applied here, the ICM, the experiment design, and the data used in this paper are introduced in Section 2. Results of mean climate states and main biases are examined through comparison with reanalysis and observations in Section 3. Sections 4 and 5 analyze the difference of the ENSO, the East Asian summer monsoon in the decaying ENSO summer year, and the IPOC effect between modeled and the observations. A summary is presented in Section 6.

2 Model and data

The ICM is an atmosphere-ocean-sea ice coupled general model without flux adjustment, which is developed at the Center for Monsoon System Research, Institute of Atmospheric Physics (CMSR/IAP), Chinese Academy of Sciences, since 2008. This model integrates the Hamburg Atmospheric General Circulation Model Version 5 (ECHAM5) (Roeckner et al. 2003) and the Nucleus for European Modeling of the Ocean Version 2.3 (NEMO 2.3) (Madec 2008) using the Ocean Atmosphere Sea Ice Soil Version 3 (OASIS3) (Valcke 2006) as the coupler. The framework of ICM is similar to the Kiel Climate Model (KCM) (Park et al. 2009) and SINTX (Gualdi et al. 2003; Luo et al. 2005). More details of ICM.V1 can be found in Huang et al. (2014).

The simulations analyzed in this paper have two different atmospheric horizontal resolutions, $3.75^\circ \times 3.75^\circ$ in ICM.V1 and $1.8^\circ \times 1.8^\circ$ in ICM.V2, but the same 19 levels in the vertical. Besides the different atmospheric horizontal resolution, the time step of the atmospheric model is changed from 2400 s in ICM.V1 to 1200 s in ICM.V2. The time step of the oceanic model is the same at 2400 s. The coupling frequency in ICM.V2 is the same as that in ICM.V1, once per 4 h. Each simulation is integrated for 1000 years. The results of higher-resolution simulation are interpolated to the lower one in the following analysis. Except for the atmospheric horizontal resolution and the time step in the atmospheric model, the rest of all settings are the same in the two versions of model simulations.

In this paper, some observation data are used with the period from 1981 to 2010. These include sea surface temperature (SST) from the Hadley Center (HadISST) (Rayner et al. 2003), the 850-hPa and 10-m winds from the National Centers for Environmental Prediction/National Center for

Atmospheric Research (NCEP) reanalysis (Kalnay et al. 1996) and the Japanese 55-year Reanalysis Project (JRA-55) (Kobayashi et al. 2015) data, respectively, and the precipitation from the Global Precipitation Climatology Project (GPCP) (Adler et al. 2003). The analyses of model simulation are based on the last 100-year output of the 1000-year integrations. All of the above observations and ICM.V2 simulation data are interpolated to the ICM.V1 grid for comparison.

3 The climatological mean state

In this section, we compare the annual and seasonal mean states of high- and low-resolution simulations with reanalysis data and observations to examine whether an increase in the horizontal resolution in the coupled model improves the representation of the mean state.

Figure 1 shows the annual mean SST from the Hadley Center (HadISST) and the difference between models and HadISST. The cold biases of SST in ICM.V1 are found in tropical, subtropical, and high-latitude regions. The mean SST simulation is improved in ICM.V2. Compared to ICM.V1, the biases in westerly wind stress decrease at 40° S in the Antarctic Circumpolar Current (ACC) area in ICM.V2, which leads to a reduction in the cold biases in the ACC area. So does the cold tongue in the tropic Pacific. Moreover, in

some ocean boundaries, the unusual positive biases are much reduced in ICM.V2 compared to those in ICM.V1. For instance, along the east coast of subtropical South and North Pacific, the biggest warm bias reaches almost 5 and 6 °C, respectively, in ICM.V1. These boundary biases are better controlled and the SST mean state simulation is better assured in ICM.V2. Meanwhile, with increasing atmospheric resolution from T31 to T63, ICM.V2 has a better simulation of mean SST in different seasons (not shown).

The distribution of model simulated precipitation and GPCP observations are shown in Fig. 2. The two model versions simulate well the main shapes of the precipitation distributions, including the Mei-Yu rain band and “C” pattern in the tropics. One common bias in the two versions of the models is an apparent double-ITCZ distribution with the precipitation overestimated over the tropical oceans. Stevens et al. (2013) indicated that increasing resolution has little contribution to decreased precipitation bias over different ECHAM versions. Our results suggest a different result. The ICM.V2 reduces precipitation in East Asia and maritime continent, which is much closer to the observations than the ICM.V2. In the central tropical Pacific, however, more precipitation appears in ICM.V2, which is worse than in ICM.V1. According to previous studies, double-ITCZ bias cannot be fully explained by the SST bias owing to the deep convection behaving differently even with a prescribed SST forcing (Zhang et al. 2007;

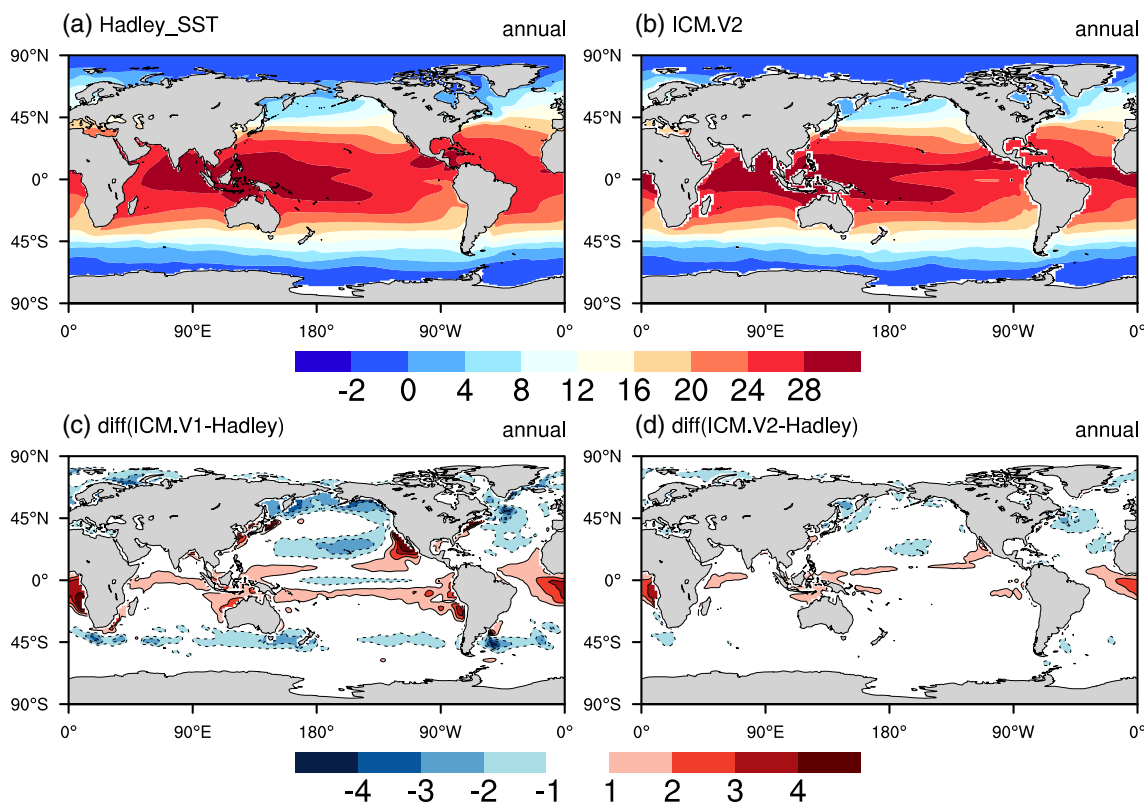


Fig. 1 Annual mean SST distribution in **a** the observation (HadISST) and **b** the simulated in ICM.V2. The difference between the simulation in ICM.V1 and the HadISST, and **d** ICM.V2 and the HadISST

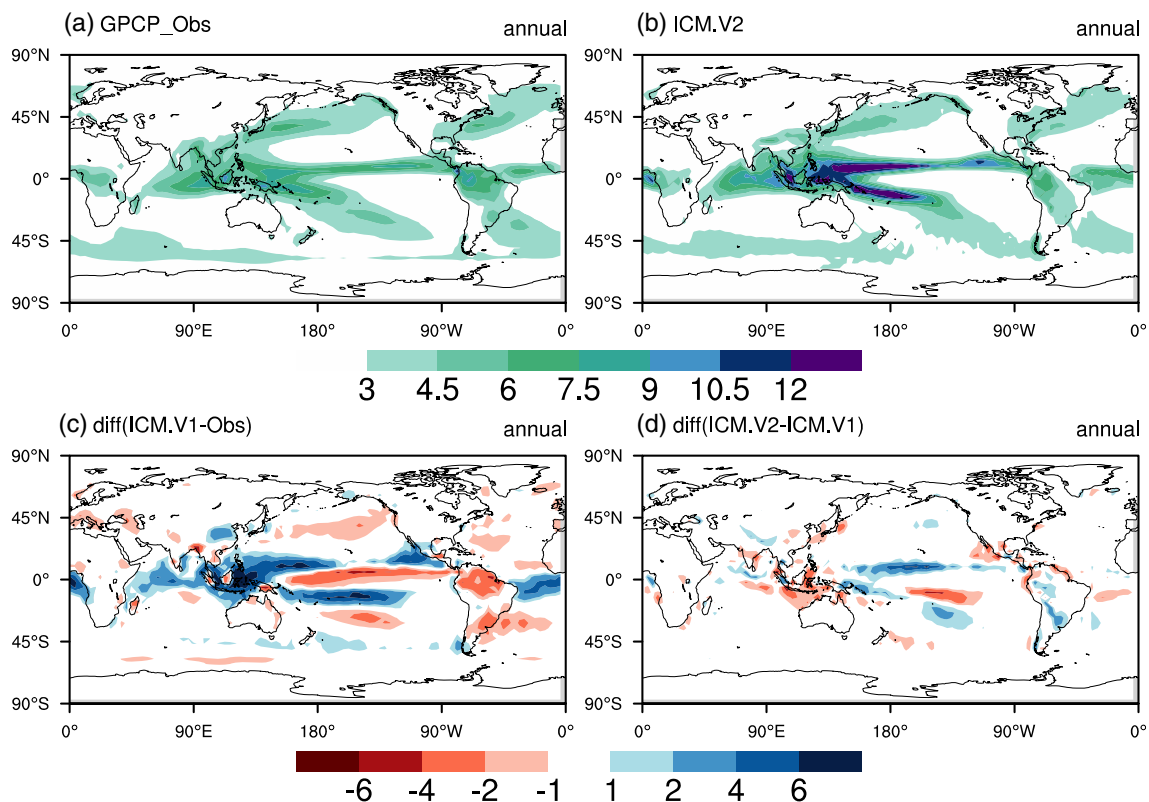


Fig. 2 Annual mean precipitation distribution in **a** the observation (GPCP) and **b** the simulated in ICM.V2. The difference between the simulation in c ICM.V1 and the GPCP, and **d** ICM.V2 and the ICM.V1

Chikira 2010), but that bias can be mitigated through modifying convective parameterization (Song and Zhang 2009; Zhang and Song 2010; Hirota et al. 2011) and using higher resolution of the ocean models with better equatorial trades (Hirota and Takayabu 2013). It will be our future work to improve ICM.V2's performance in precipitation simulation.

To quantify the spatial distribution in two model versions compared to observations, Fig. 3a shows the Taylor plots of SST and precipitation in annual mean and different seasons between the simulated and observations. The red and black colors represent ICM.V1 and ICM.V2, respectively. From the Taylor plots, both model versions have better performance in SST than precipitation. Meanwhile, the black dots, which represent the high-resolution model version, always show greater correlations and less standardized deviations with observations in annual and seasonal means (numbers 1 to 5 in Fig. 3). That means some improvements of the skill of the models in reproducing the spatial patterns of SST and precipitation with increasing horizontal resolution, and the higher resolution of ICM has a better performance in simulating the climate state of SST and precipitation.

Figure 3b displays the Taylor plots of 850-hPa meridional, zonal wind, and the amplitude of wind in annual mean and different seasons between the simulated and observations. Similar to Fig. 3a, with increasing horizontal resolution, the climate mean states of 850-hPa winds have improved to some

extent. The ICM.V2 simulation has a higher correlation with NCEP reanalysis data than the ICM.V1 simulation.

4 The inter-annual variability of ENSO

In the Pacific Ocean, the dominant inter-annual mode is the ENSO. Many previous studies showed that the seasonal cycle of the equatorial Pacific SST plays a dominant role in the development of El Niño events (Wang and Picaut 2004; Guilyardi 2006). The seasonal cycle of SST deviation from the annual mean over the equatorial Pacific in observation and two model simulations is shown in Fig. 4. Compared to the observations, both model versions simulate the seasonal cycle similar to the observations, and the spatial correlation with the observation is 0.67 in both simulations. The spatial structure, however, in the higher-resolution version resembles more closely that in the Hadley SST. At around 150° W, ICM.V1 has an unreal positive anomaly in May and a negative anomaly in October. In ICM.V2, the structure has a better match with the observations, with the large positive and negative value center concentrated between 120° W and 90° W.

The more realistic simulation in the spatial structure of the seasonal cycle of SST in the equatorial Pacific ensures a better simulation of ENSO in the high-resolution version. The inter-annual variance of tropical Pacific SST is shown in Fig. 5. The

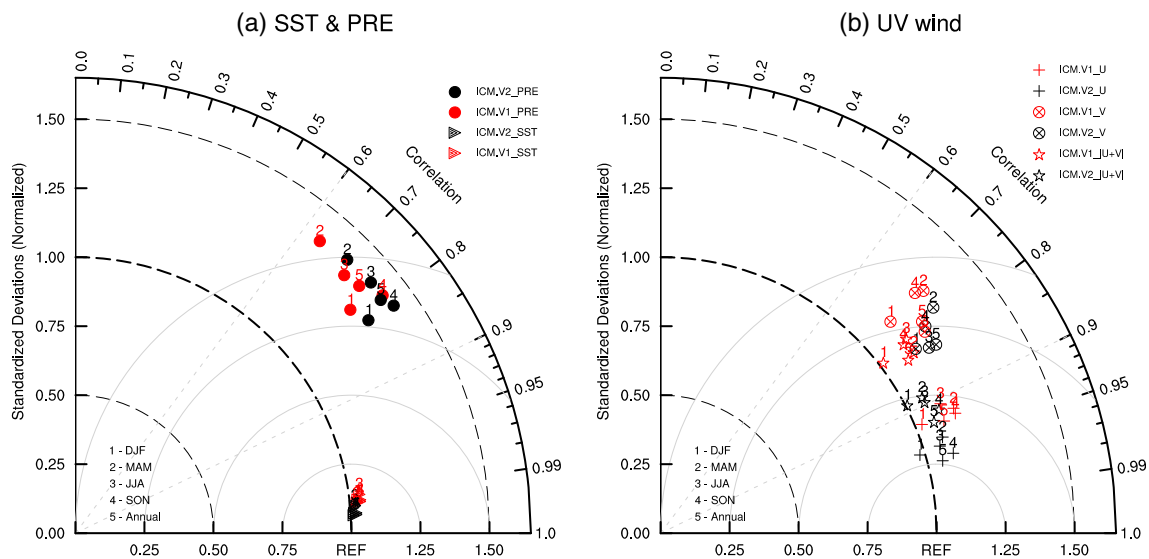


Fig. 3 Taylor diagrams showing a skill score for the model reproducibility of the **a** SST and precipitation pattern and the **b** 850-hPa meridional and zonal wind pattern, based on the monthly global data for each season and annual mean (represented by numbers 1 to 5). The

pattern correlation with the observation pattern (from 1981 to 2010) is shown as the azimuthal position, while the radial distance indicates the standard deviation

large variance is present along the equatorial Pacific in the observations and model simulations. Specifically, the large variance region extends excessively westward in ICM.V1, which to some extent has been subdued in ICM.V2.

The power spectrum of Niño3 SST is shown in Fig. 5b. The period of ENSO is around 3.75 years in the observations. Both versions of models can represent well the observed spectrum. In comparison, the period has improved in the high-resolution version. The peak is around 3.33 years in ICM.V2, which is closer to the observation compared to that in ICM.V1 (2.7 years). The improvement of the ENSO variability in ICM.V2 could be associated with the improved climatological SST in the high-resolution model version (Fig. 1 and Fig. 2).

5 The western North Pacific summer climate

In summertime, the most important characteristic is the Mei-Yu rain band over East Asia. The abundant moisture for the Mei-Yu comes from the tropical ocean through the summer monsoon winds. The summer monsoon variability has a great impact on the economy because it brings flood or drought disaster (Zhou et al. 2014). So the summer monsoon is a vital target in climate model simulations. In this section, we evaluate the performance of the two versions of model simulations in this aspect.

In Fig. 6a–c, the summer precipitation and 850-hPa wind over the East Asian and the western North Pacific are shown.

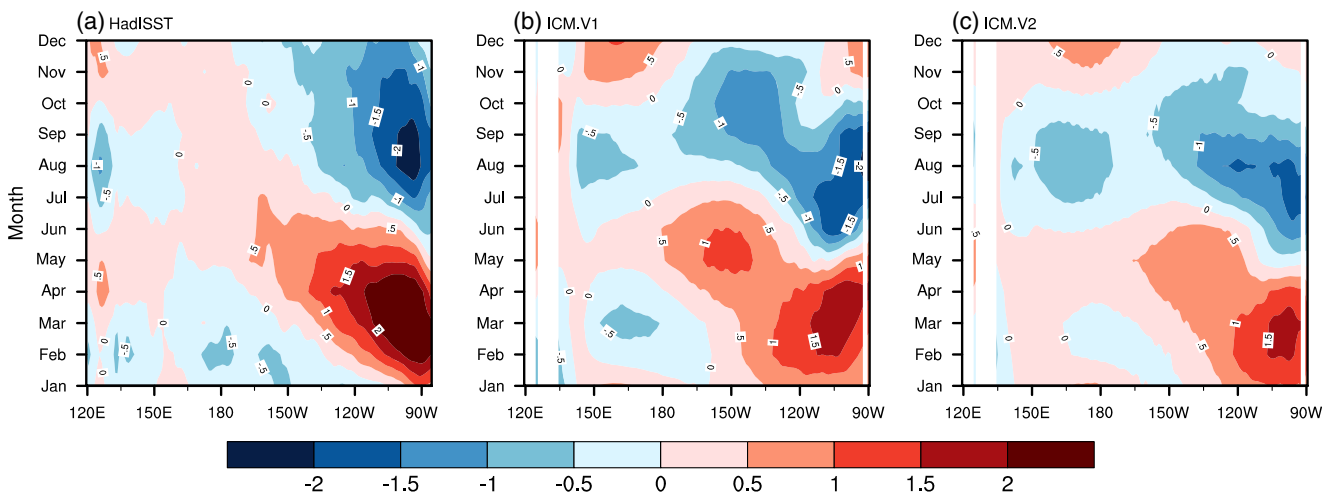


Fig. 4 **a** Observed, **b** ICM.V1, and **c** ICM.V2 modeled seasonal cycle of SST deviation from the annual mean (°C) over the equatorial Pacific

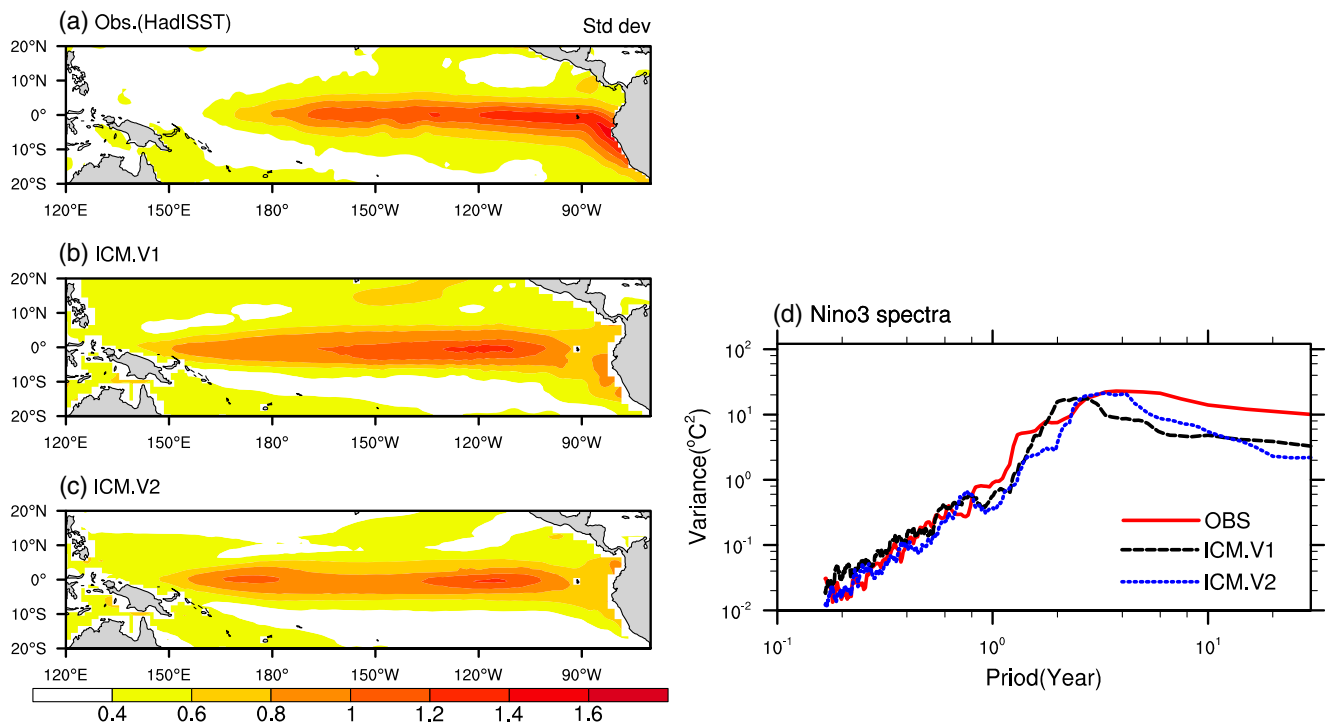


Fig. 5 The inter-annual variance of SST in the tropical Pacific in **a** the observations (HadISST), **b** ICM.V1, and **c** ICM.V2. **d** Power spectrum analysis, in which the red curve represents the observation, the black dash

curve represents the simulation of ICM.V1, and the blue dot curve represents the simulation of ICM.V2

We can see a long rain band lying over the tropical ocean, east of China and Korea to the Japan Ocean, associated with a large anticyclone in the observations (Fig. 6a). The two versions of models can well simulate the pattern of rain band (Fig. 6b, c). In

comparison, the rainfall in the rain band of ICM.V1 simulation is less than the observations, especially over the Japan Ocean. Moreover, because the simulated western North Pacific anticyclone is located north- and eastward, the rain band shifts to the

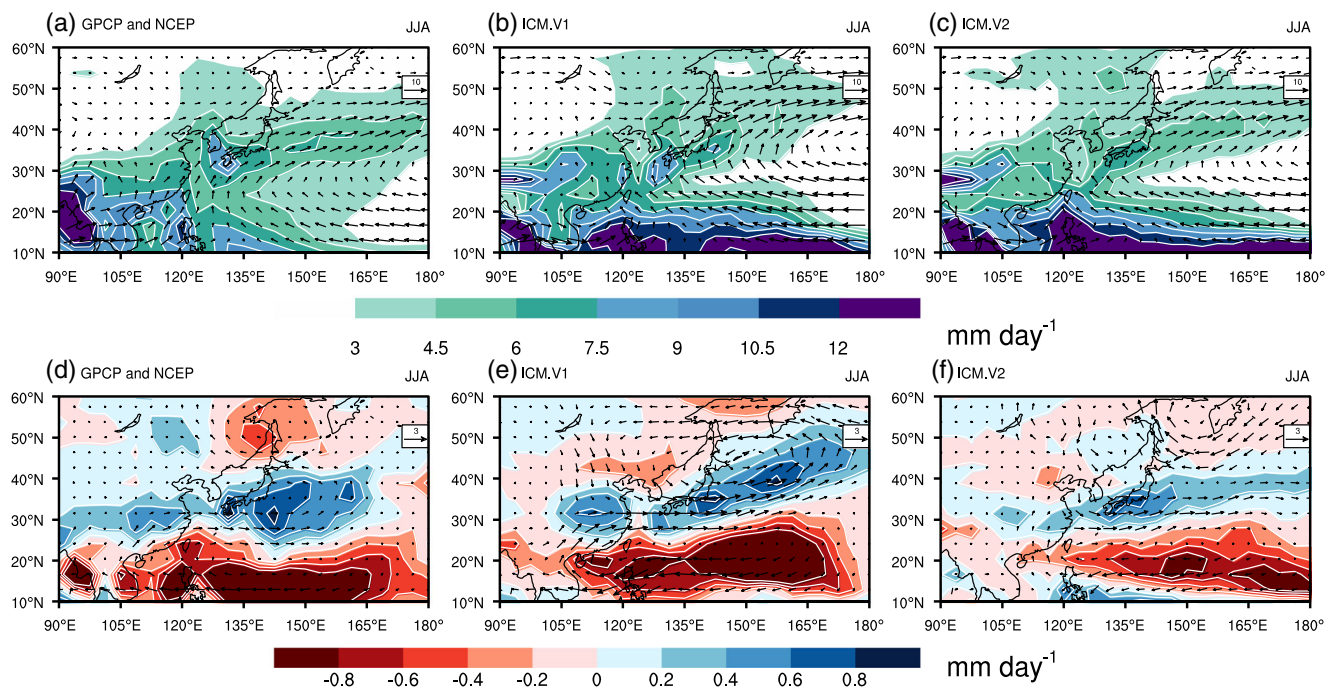


Fig. 6 The summer climatological precipitation (shaded; mm/day) and 850-hPa wind (vector; m/s) from **a** GPCP and NCEP, **b** ICM.V1, and **c** ICM.V2. The PJ patterns in **d** GPCP and NCEP, **e** ICM.V1, and **f** ICM.V2

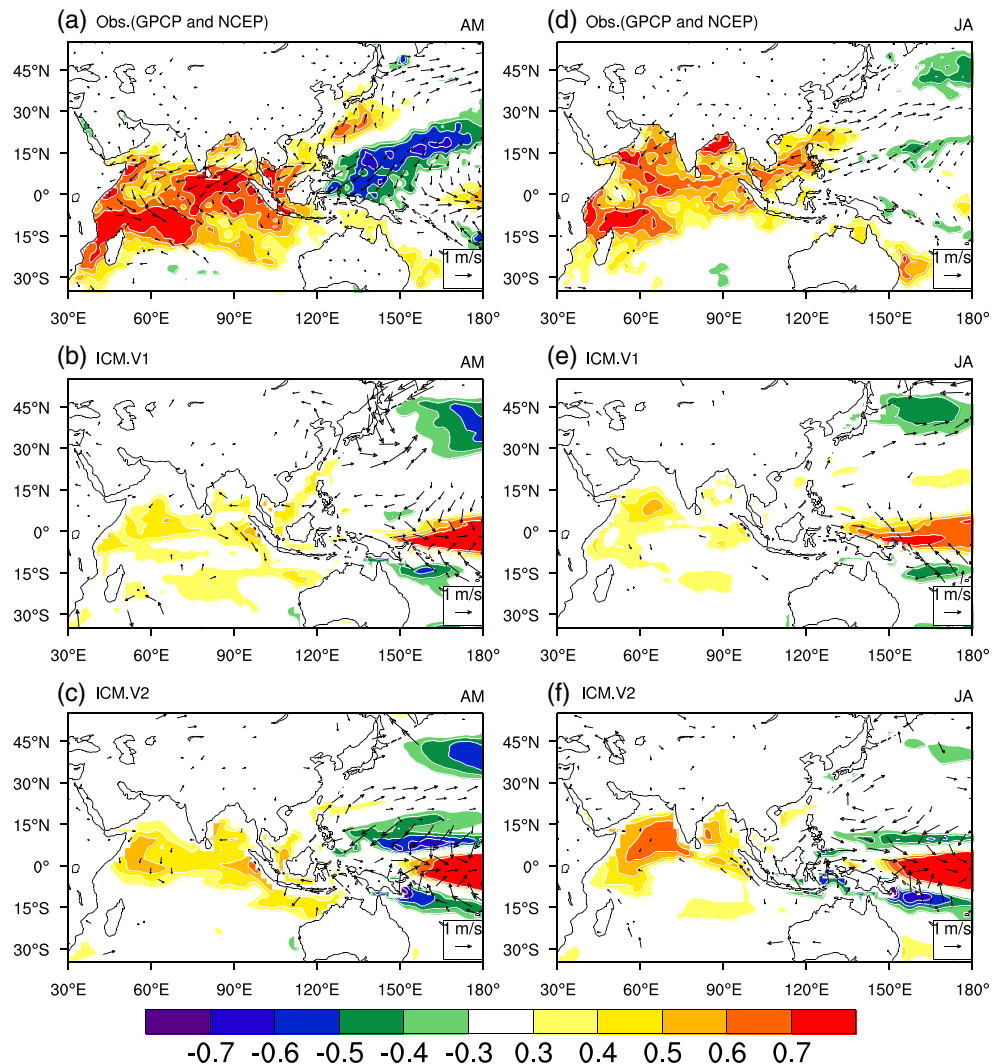
north and east. This bias has lessened in ICM.V2 in which the location and pattern of the anticyclone and the rain band are much closer to the observations over East Asia.

Over East Asia and the western North Pacific, the inter-annual variability of summer circulation is characterized by the Pacific-Japan (PJ) teleconnection with a distinct triple meridional structure. According to Kosaka et al. (2013), the PJ pattern is calculated through an empirical orthogonal function (EOF) analysis applied to the summer (JJA) 850-hPa vorticity anomaly (0–60° N, 100–160° E), and then the principal component (PC1) is regressed on the precipitation and 850-hPa wind anomaly. The obtained PJ pattern is shown in Fig. 6d–f. We can see a clear triple meridional structure with positive, negative, positive precipitation anomalies over East Asia associated with anticyclone, cyclone, anticyclone wind anomalies, respectively, in the observations (Fig. 6d). In ICM.V1, the magnitude of the simulated precipitation matches well with the observations. However, the orientation of the precipitation pattern shifts northward at the subtropical latitude. Moreover,

the corresponding 850-hPa wind pattern has a great deviation as well and the north branch of the anticyclone anomaly at high latitude is not visible. The performance of ICM.V2 in simulating the PJ pattern has great improvement. The location and magnitude of the circulation anomaly agree well with the observations although the magnitude of precipitation is slightly reduced.

As we showed above, the simulation of ENSO is improved in ICM.V2, including the period and SST anomaly pattern. How would the ENSO influence the western North Pacific summer climate? In the decaying summer of El Niño, an anomalous anticyclone often forms over the western North Pacific (WPAC). This WPAC is regarded as a bridge linking the ENSO and western North Pacific summer climate (Wang et al. 2000). Moreover, researches have emphasized the function of the Indian Ocean (Yang et al. 2007; Wu et al. 2009; Xie et al. 2009). According to the recent research by Xie et al. (2016), the IPOC effect explained that in the ENSO decaying summer the Indian Ocean and western Pacific Ocean play

Fig. 7 Correlation of April–May (AM) and July–August (JA) SST (colors) in the **a** observation, **b** ICM.V1, and **c** ICM.V2 with DJF(0) Nino3 index and regression of April–May (AM) and July–August (JA) 10-m winds (vectors; m/s) in the **d** observation, **e** ICM.V1, and **f** ICM.V2 with DJF(0) Nino3 index



different roles in early and late summer. In the decaying early summer of ENSO, the WPAC and Northwest Pacific cooling are coupled via wind-evaporation-SST (WES) feedback (Wang et al. 2000). During the late summer, the mechanism changes to the interaction of the WPAC and north Indian Ocean warming. So in our following analysis, we discuss ENSO impacts on the western North Pacific summer climate in the early and late summer.

Similar to the results of Xie et al. (2016), the observations show great cooling in the Northwest Pacific in April–May (AM) (Fig. 7a), which is associated with an anomalous anticyclone in low-level circulation. But in July–August (JA) (Fig. 7d), the cooling basically disappears and the Indian Ocean warming takes charge. The WPAC is formed through the whole summertime and reaches larger amplitude in late summer. In the low-resolution model, the Northwest Pacific cooling is much weaker than observation in AM (Fig. 7b), and the north Indian Ocean warming does not reach the observed magnitude as well (Fig. 7c). In the simulation of the high-resolution version, the Northwest Pacific cooling in AM (Fig. 7e) and the north Indian Ocean warming (Fig. 7f) have great improvement, with the associated 850-hPa wind anomaly featuring distinct WPAC, which is quite close to the observations. Nonetheless, the magnitude of the Northwest Pacific cooling in AM and the north Indian Ocean warming is still lower than the observations, leading to the WPAC located somewhat eastward. Hence, the IPOC effect plays an important role in the ENSO-related western North Pacific summer climate.

Generally speaking, the high-resolution version is a better choice to investigate the ENSO and its impact on the western North Pacific summer climate.

Besides the IPOC effect, many previous studies have mentioned that Pacific decadal oscillation (PDO) plays an important role in modulating the ENSO-EASM relationship (Feng et al. 2014; Dong and Dai 2015; Song and Zhou 2015). PDO is the leading mode in the North Pacific Ocean (Mantua et al. 1997). As Feng et al. (2014) mentioned, PDO in a different phase may modulate the ENSO-EASM relationship through the decay speed of El Niño during 1957–2011, and during the high PDO phase, El Niño decays slowly and has a strong anchor to the north Indian Ocean warming, which leads to the anomalous EASM. So next, we discuss the difference of simulation of the PDO between models and observation.

We apply the EOF analysis to the SST anomaly 20° N, and the PDO index is defined using the standardized PC1. Figure 8 shows the regression of the PDO index on SST in the Pacific Ocean. In Fig. 8a, a dipole pattern of the SST anomaly lies over the North Pacific with the warm center anomaly in the center-east tropical Pacific and the cool center anomaly at around 20–40° N. The PDO simulated in ICM.V1 (Fig. 8b) has a great difference from the observations, especially the tropical branch, with the warm center anomaly too cooler and the cool center anomaly slightly shifted westward. In contrast, the performance of ICM.V2 in simulating the PDO shows great advantage in both the pattern and magnitude (Fig. 8c).

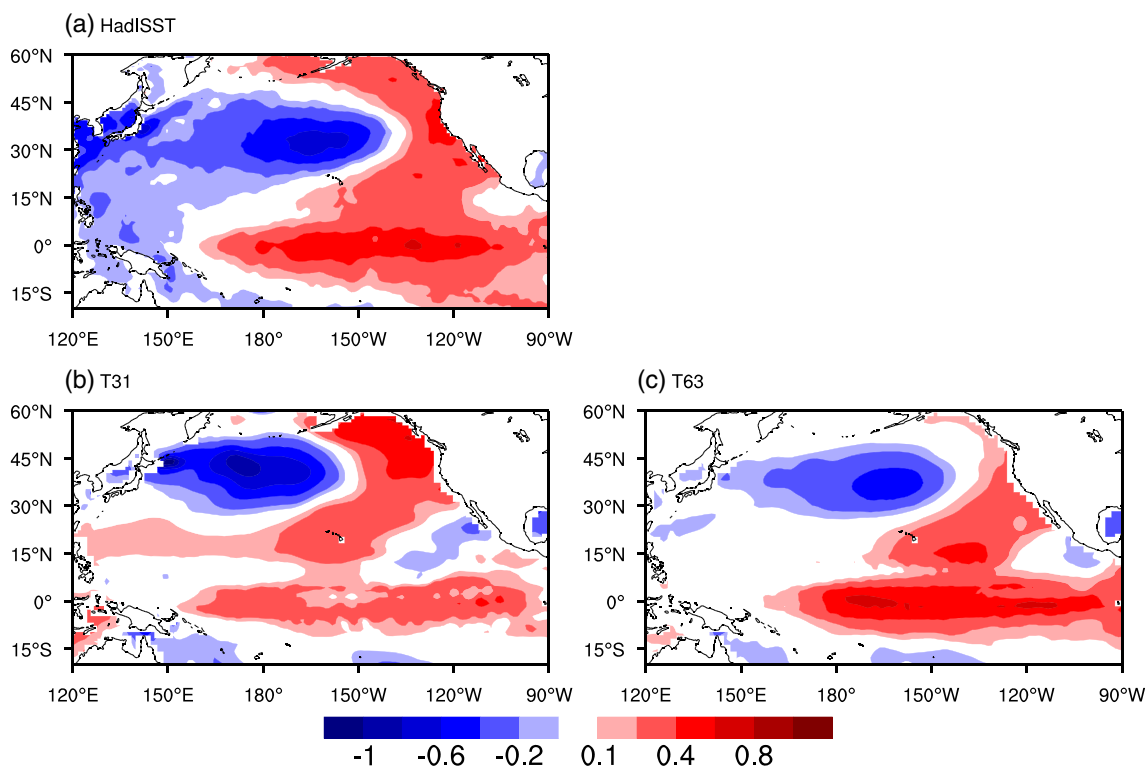


Fig. 8 The regression of the PDO index on SST (shade; °C) in the Pacific Ocean from **a** Hadley, **b** ICM.V1, and **c** ICM.V2

The warm center anomaly is concentrated in the tropical Pacific, and the magnitude is closer to observation than ICM.V1. In ICM.V2's simulation, the PDO (Fig. 8) and the period of ENSO (becomes longer which is analyzed in Section 4) both are relatively similar to the observation, and the IPOC effect is greater than ICM.V1. These processes are well matched with the results of Feng et al. (2014). Therefore, the better simulations of the PDO and IPOC effect in a higher-resolution model may have a certain degree of contribution to the better performance over the western North Pacific summer climate.

6 Conclusions

This study analyzes whether and to what degree the performance of ICM benefits from the horizontal resolution increase from ICM.V1 to ICM.V2. ICM is an ocean-atmosphere coupled model with the atmospheric model ECHAM5.3 (Roeckner et al. 2003) and the ocean part NEMO2.3 (Madec 2008) coupled by Oasis3 (Valcke 2006). Both the simulations in high- and low-resolution versions of the model are compared to reanalysis and observation data from aspects of annual mean states in SST and precipitation. The results show that the SST simulation has obvious improvement in the high-resolution version, including the reduction in the cold bias in the tropic Pacific, which is a common bias in coupled model simulations, and the ocean boundary biases. This may result from the improved surface wind simulation in the atmospheric model. On the other side, the simulation in precipitation is still a great challenge in GCM. But, there is relative improvement in the performance of precipitation simulation in ICM.V2 over the Maritime Continent and East Asia, where the low-resolution version model has simulated excessively high rainfall. Moreover, we find that the high-resolution version shows greater correlations with and less standardized deviations from observations in annual to seasonal mean SST, precipitation, and winds. That means some improvements of the skill of the models in reproducing the spatial patterns of SST, precipitation, and winds with increasing horizontal resolution. The higher-resolution ICM has a better performance in simulating the climate state of SST, precipitation, and winds. The East Asian summer monsoon has quite an improvement with respect to precipitation and the associated circulation pattern. In addition, the dominant inter-annual mode over the western North Pacific, the PJ pattern, is reproduced better as well, especially with respect to the shape. But the magnitude is still too small.

In the performance of inter-annual variability ENSO, through comparing the season cycle of equatorial Pacific SST and the period and pattern of ENSO, the high-resolution version shows better performance than the low-

resolution one. That indicates that the high resolution has a better simulation of ENSO. Then, we investigate the impact of ENSO on the western North Pacific summer climate. With the increasing horizontal resolution, ICM.V2 has shown large promotion on the Northwest Pacific cooling in early summer, which via WES feedback intensifies the WPAC (Wang et al. 2000), and on the north India warming (Wu et al. 2009; Xie et al. 2009) in late summer which strengthens the WPAC and affects the western Pacific summer climate. Overall, the high-resolution version model shows a better performance in simulating ENSO and its impact on the western Pacific summer climate. The better simulation of the IPOC effect which has better performance on the ENSO-related western North Pacific summer climate in the high-resolution model is one reason; moreover, we investigate the other plausible reason and find that the high-resolution model has an improved simulation of PDO. The warm center anomaly is more concentrated on the center-east tropical Pacific, and the cold center anomaly is more eastward to the center of the North Pacific in the high-resolution version, resembling more the observations than in the low-resolution version. Additionally, according to previous studies, many other factors, such as the spring North Atlantic Oscillation (NAO; Wu et al. 2012) and the East Asian winter monsoon (EAWM; Feng and Chen 2014), may have an impact on the ENSO-EASM relationship, which needs a detailed investigation in our future study. Meanwhile, we also should realize that the ENSO-EASM relationship is unstable (Wang 2002; Song and Zhou 2015).

Based on the present analyses, it can be concluded that the high-resolution ICM has a large improvement in the performance of mean state and western North Pacific summer climate. It is a better choice to use the ICM.V2 version of ICM to make further investigation on other research topics. But still, more assessments and improvements should be taken to study the possible biases on simulating other climate systems, including time scales ranging from inter-annual to inter-decadal.

Acknowledgements This work was supported by the National Natural Science Foundation of China (41425019 and 41661144016) and the Public Science and Technology Research Funds Projects of Ocean (201505013).

References

- Adler RF et al (2003) The version-2 global precipitation climatology project (GPCP) monthly precipitation analysis (1979-present). *J Hydrometeorol* 4:1147–1167. [https://doi.org/10.1175/1525-7541\(2003\)004](https://doi.org/10.1175/1525-7541(2003)004)
- Bryan FO, Tomas R, Dennis JM, Chelton DB, Loeb NG, McClean JL (2010) Frontal scale air-sea interaction in high-resolution coupled climate models. *J Clim* 23:6277–6291. <https://doi.org/10.1175/2010JCLI3665.1>
- Chikira M (2010) A cumulus parameterization with state-dependent entrainment rate. Part II: Impact on climatology in a general circulation

- model. *J Atmos Sci* 67:2194–2211. <https://doi.org/10.1175/2010JAS3317.1>
- Delworth TL et al (2012) Simulated climate and climate change in the GFDL CM2.5 high-resolution coupled climate model. *J Clim* 25: 2755–2781. <https://doi.org/10.1175/jcli-d-11-00316.1>
- Dong B, Dai AG (2015) The influence of the interdecadal Pacific oscillation on temperature and precipitation over the globe. *Clim Dyn* 45: 2667–2681. <https://doi.org/10.1007/s00382-015-2500-x>
- Feng J, Chen W (2014) Interference of the East Asian winter monsoon in the impact of ENSO on the East Asian summer monsoon in decaying phases. *Adv Atmos Sci* 31:344–354. <https://doi.org/10.1007/s00376-013-3118-8>
- Feng J, Wang L, Chen W (2014) How does the East Asian summer monsoon behave in the decaying phase of El Niño during different PDO phases? *J Clim* 27:2682–2698. <https://doi.org/10.1175/Jcli-D-13-00015.1>
- Gent PR, Yeager SG, Neale RB, Levis S, Bailey DA (2010) Improvements in a half degree atmosphere/land version of the CCSM. *Clim Dyn* 34:819–833. <https://doi.org/10.1007/s00382-009-0614-8>
- Gualdi S, Navarra A, Guilyardi E, Delecluse P (2003) Assessment of the tropical Indo-Pacific climate in the SINTEX CGCM. *Ann Geophys-Italy* 46:1–26
- Guilyardi E (2006) El Niño-mean state-seasonal cycle interactions in a multi-model ensemble. *Clim Dyn* 26:329–348. <https://doi.org/10.1007/s00382-005-0084-6>
- Hertwig E, von Storch JS, Handorf D, Dethloff K, Fast I, Krismer T (2015) Effect of horizontal resolution on ECHAM6-AMIP performance. *Clim Dyn* 45:185–211. <https://doi.org/10.1007/s00382-014-2396-x>
- Hirota N, Takayabu YN (2013) Reproducibility of precipitation distribution over the tropical oceans in CMIP5 multi-climate models compared to CMIP3. *Clim Dyn* 41:2909–2920. <https://doi.org/10.1007/s00382-013-1839-0>
- Hirota N, Takayabu YN, Watanabe M, Kimoto M (2011) Precipitation reproducibility over tropical oceans and its relationship to the double ITCZ problem in CMIP3 and MIROC5 climate models. *J Clim* 24: 4859–4873. <https://doi.org/10.1175/2011JCLI4156.1>
- Hu KM, Huang G, Wu RG (2013) A strengthened influence of ENSO on August high temperature extremes over the southern Yangtze River valley since the late 1980s. *J Clim* 26:2205–2221. <https://doi.org/10.1175/JCLI-D-12-00277.1>
- Huang P, Wang P, Hu K, Huang G, Zhang Z, Liu Y, Yan B (2014) An introduction to the integrated climate model of the Center for Monsoon System Research and its simulated influence of El Niño on East Asian-western North Pacific climate. *Adv Atmos Sci* 31: 1136–1146. <https://doi.org/10.1007/s00376-014-3233-1>
- Jiang T, Kundzewicz ZW, Su B (2008) Changes in monthly precipitation and flood hazard in the Yangtze River basin, China. *Int J Climatol* 28:1471–1481. <https://doi.org/10.1002/joc.1635>
- Kalnay E et al (1996) The NCEP/NCAR 40-year reanalysis project. *B Am Meteorol Soc* 77:437–471. [https://doi.org/10.1175/1520-0477\(1996\)077](https://doi.org/10.1175/1520-0477(1996)077)
- Kobayashi S et al (2015) The JRA-55 reanalysis: general specifications and basic characteristics. *J Meteorol Soc Jpn* 93:5–48. <https://doi.org/10.2151/jmsj.2015-001>
- Kosaka Y, Xie SP, Lau NC, Vecchi GA (2013) Origin of seasonal predictability for summer climate over the northwestern Pacific. *P Natl Acad Sci USA* 110:7574–7579. <https://doi.org/10.1073/pnas.1215582110>
- Luo JJ, Masson S, Roeckner E, Madec G, Yamagata T (2005) Reducing climatology bias in an ocean-atmosphere CGCM with improved coupling physics. *J Clim* 18:2344–2360. <https://doi.org/10.1175/Jcli3404.1>
- Madec G (2008) NEMO ocean engine. Note du pole de modelisation 27, Institut Pierre-Simon Laplace 193 pp
- Mantua NJ, Hare SR, Zhang Y, Wallace JM, Francis RC (1997) A Pacific interdecadal climate oscillation with impacts on salmon production. *B Am Meteorol Soc* 78:1069–1079. [https://doi.org/10.1175/1520-0477\(1997\)078<1069:Apicow>2.0.Co;2](https://doi.org/10.1175/1520-0477(1997)078<1069:Apicow>2.0.Co;2)
- McClellan JL et al (2011) A prototype two-decade fully-coupled fine-resolution CCSM simulation. *Ocean Model* 39:10–30. <https://doi.org/10.1016/j.ocemod.2011.02.011>
- Park W, Keenlyside N, Latif M, Ströh A, Redler R, Roeckner E, Madec G (2009) Tropical Pacific climate and its response to global warming in the Kiel climate model. *J Clim* 22:71–92. <https://doi.org/10.1175/2008jcli2261.1>
- Rayner NA et al (2003) Global analyses of sea surface temperature, sea ice, and night marine air temperature since the late nineteenth century. *J Geophys Res-Atmos* 108. <https://doi.org/10.1029/2002jd002670>
- Rodwell MJ, Hoskins BJ (2001) Subtropical anticyclones and summer monsoons. *J Clim* 14:3192–3211. [https://doi.org/10.1175/1520-0442\(2001\)014,3192:SAASM.2.0.CO;2](https://doi.org/10.1175/1520-0442(2001)014,3192:SAASM.2.0.CO;2)
- Roeckner E, et al (2003) The atmospheric general circulation model ECHAM5. PART I: Model description. Report 349, Max Planck Institute for Meteorology 140 pp
- Roeckner E et al (2006) Sensitivity of simulated climate to horizontal and vertical resolution in the ECHAM5 atmosphere model. *J Clim* 19: 3771–3791. <https://doi.org/10.1175/Jcli3824.1>
- Sakamoto TT et al (2012) MIROC4h—a new high-resolution atmosphere-ocean coupled general circulation model. *J Meteorol Soc Jpn* 90:325–359
- Song XL, Zhang GJ (2009) Convection parameterization, tropical Pacific double ITCZ, and Upper-Ocean biases in the NCAR CCSM3. Part I: Climatology and Atmospheric Feedback. *J Clim* 22:4299–4315. <https://doi.org/10.1175/2009JCLI2642.1>
- Song F, Zhou T (2015) The crucial role of internal variability in modulating the decadal variation of the east Asian summer monsoon–ENSO relationship during the twentieth century. *J Clim* 28:7093–7107. <https://doi.org/10.1175/jcli-d-14-00783.1>
- Stevens B, Giorgetta M, Esch M, Mauritsen T, Cruieger T, Rast S, Salzmann M, Schmidt H, Bader J, Block K, Brokopf R, Fast I, Kinne S, Kornblueh L, Lohmann U, Pincus R, Reichler T, Roeckner E (2013) Atmospheric component of the MPI-M earth system model: ECHAM6. *J Adv Model Earth Syst* 5(2):146–172
- Valcke S (2006) OASIS3 user guide. PRISM Tech Rep 3:64 pp
- Wang HJ (2002) The instability of the East Asian summer monsoon–ENSO relations. *Adv Atmos Sci* 19:1–11
- Wang CZ, Picaut J (2004) Understanding ENSO physics—a review. *Geophys Monogr Ser* 147:21–48
- Wang B, Wu RG, Fu XH (2000) Pacific-East Asian teleconnection: how does ENSO affect East Asian climate? *J Clim* 13:1517–1536. [https://doi.org/10.1175/1520-0442\(2000\)013<1517:Peathd>2.0.Co;2](https://doi.org/10.1175/1520-0442(2000)013<1517:Peathd>2.0.Co;2)
- Wang B, Wu RG, Li T (2003) Atmosphere-warm ocean interaction and its impacts on Asian-Australian monsoon variation. *J Clim* 16: 1195–1211. [https://doi.org/10.1175/1520-0442\(2003\)16<1195:Aoiaii>2.0.Co;2](https://doi.org/10.1175/1520-0442(2003)16<1195:Aoiaii>2.0.Co;2)
- Williamson DL, Kiehl JT, Hack JJ (1995) Climate sensitivity of the Near community climate model (Ccm2) to horizontal resolution. *Clim Dyn* 11:377–397. <https://doi.org/10.1007/Bf00209513>
- Wu B, Zhou TJ, Li T (2009) Seasonally evolving dominant interannual variability modes of East Asian climate. *J Clim* 22:2992–3005. <https://doi.org/10.1175/2008JCLI2710.1>
- Wu ZW, Li JP, Jiang ZH, He JH, Zhu XY (2012) Possible effects of the North Atlantic oscillation on the strengthening relationship between the East Asian summer monsoon and ENSO. *Int J Climatol* 32:794–800
- Xie SP, Hu KM, Hafner J, Tokinaga H, Du Y, Huang G, Sampe T (2009) Indian Ocean capacitor effect on Indo-western Pacific climate

- during the summer following El Nino. *J Clim* 22:730–747. <https://doi.org/10.1175/2008JCLI2544.1>
- Xie SP, Kosaka Y, Du Y, Hu KM, Chowdary J, Huang G (2016) Indo-western Pacific ocean capacitor and coherent climate anomalies in post-ENSO summer: a review. *Adv Atmos Sci* 33:411–432. <https://doi.org/10.1007/s00376-015-5192-6>
- Yang JL, Liu QY, Xie SP, Liu ZY, Wu LX (2007) Impact of the Indian Ocean SST basin mode on the Asian summer monsoon. *Geophys Res Lett* 34. <https://doi.org/10.1029/2006gl028571>
- Zhang GJ, Song XL (2010) Convection parameterization, tropical Pacific double ITCZ, and Upper-Ocean biases in the NCAR CCSM3. Part II: Coupled Feedback and the Role of Ocean Heat Transport. *J Clim* 23: 800–812. <https://doi.org/10.1175/2009JCLI3109.1>
- Zhang RH, Sumi A, Kimoto M (1999) A diagnostic study of the impact of El Nino on the precipitation in China. *Adv Atmos Sci* 16:229–241. <https://doi.org/10.1007/Bf02973084>
- Zhang XH, Lin WY, Zhang MH (2007) Toward understanding the double intertropical convergence zone pathology in coupled ocean-atmosphere general circulation models. *J Geophys Res-Atmos*: 112. <https://doi.org/10.1029/2006jd007878>
- Zhou TJ, Ma SM, Zou LW (2014) Understanding a hot summer in central eastern China: summer 2013 in context of multimodel trend analysis. *B Am Meteorol Soc* 95:S54–S57